Mechanical Testing and Diagnosis
ISSN 2247 – 9635, 2011 (I), Volume 1, 40-47

BIODIESEL INFLUENCE ON DIESEL ENGINE EMISSION

Breda KEGL, Stanislav PEHAN

University of Maribor, Maribor, Slovenia, b, 2000 Maribor, SLOVENIA
E-mail: breda.kegl@uni-mb.si, stanislav.pehan@uni-mb.si

ABSTRACT

This paper discusses the influence of the neat biodiesel made from rapeseed oil on the bus diesel engine with injection M system. Running the diesel engine the relationships among fuel properties, injection and combustion characteristics and harmful emission, are investigated. The engine characteristics by experiments and numerical simulation are compared.

The influences of biodiesel on the injection pressure, injection timing, ignition delay, in cylinder gas pressure and temperature, heat release rate, exhaust gas temperatures, harmful emissions, specific fuel consumption, and on engine power are analyzed.

The results obtained with biodiesel are compared to those obtained with mineral diesel. Special attention is given to explanations of higher NO_x emission in spite of lower in cylinder gas temperature.

Keywords:biodiesel, NO_x emission, heat release rate

1. INTRODUCTION

In general, biofuels may offer an excellent opportunity to reduce some of the harmful emissions without expensive engine modifications. Since vegetable oils satisfy the major diesel engine requirements their suitability as alternative fuel has frequently been investigated in recent years. For example, investigations of used orange oil shows that orange oil exhibits an increased ignition delay, higher combustion duration, and higher heat release rate, compared to mineral diesel [1]. This results in reducing HC, CO and smoke emissions meanwhile the NO_x emission are higher [2, 3].

Among all biofuels for diesel engines, biodiesel is a very promising fuel because it is a sulfur-free, non-toxic, oxygenated, renewable, and more than 90% biodiesel can be biodegradable within 21 days [4]. Biodiesel has higher cetane number than mineral diesel, no aromatics, almost no sulfur, and contains more oxygen by weight. Biodiesel fuel with a cetane number similar to the diesel fuel produced higher NO_x emissions than the diesel fuel.

Biodiesel has higher density, viscosity, surface tension, sound velocity, and bulk modulus of elasticity. This affects the fuelling, injection timing, and fuel spray and

Mechanical Testing and Diagnosis, ISSN 2247 – 9635,2011 (I), Volume 1, 40-47

consequently the emission characteristics [5]. On the basis of the physical properties of the biodiesel, it can be summarized that the advantages of the biodiesel are shorter ignition delay due to a higher cetane number and an enhanced combustion process caused by oxygen in the biodiesel. Biodiesel has lower heating value than mineral diesel and causes some loss of power. Therefore, it is necessary to increase the fuel amount to be injected into the combustion chamber. This will cause longer injection duration due to change in the injection timing.

The objective was to identify as much as possible the dependences among fuel properties, the most important injection and combustion characteristics, harmful engine emissions, and other engine performances. Special attention is devoted to dependences among injection timing, in-cylinder gas temperature and NO_x emission.

2. NUMERICAL SIMULATION

The paper outlines briefly the fundamentals of the employed software AVL BOOST v2009.1 and the sub-models chosen for this work. The employed mathematical model is based on the first law of thermodynamics [6], which can be (for an internal combustion piston engine) written as

$$\frac{d(m_c \cdot u)}{d\alpha} = -p_c \cdot \frac{dV}{d\alpha} + \frac{dQ_f}{d\alpha} - \sum \frac{dQ_w}{d\alpha} - h_{BB} \cdot \frac{dm_{BB}}{d\alpha} \quad \textbf{(1)}$$

Basically, for the high pressure cycle this law states that the change of the internal energy in the cylinder $\left(d(m_c \cdot u)/d\alpha\right)$ is equal to the sum of piston work $\left(-p_c(dV/d\alpha)\right)$, the conversion of chemical energy to the thermal energy $(dQ_f/d\alpha)$, heat transfer $(-\Sigma(dQ_W/d\alpha))$, and the enthalpy flow due to blow-by $(-h_{BB}(dm_{BB}/d\alpha))$. The conversion of chemical energy to the thermal energy represents the heat release. In equation (1) the symbol α denotes the angle of the crankshaft rotation, m_c is the mass of the mixture in the cylinder, u is the specific internal energy, p_c is the in-cylinder pressure, V is the cylinder volume Q_f is the fuel energy, Q_W the heat transfer through the liner, h_{BB} and $h \cdot m_{BB}$ are the enthalpy and mass of the mixture that escapes through the gap between the piston and the liner, respectively. With the in-cylinder gas pressure p_c and the working displacement of one piston, V_D, the indicated mean effective pressure p_i can be determined over the whole cycle duration as follows: $p_i = (1/V_D)\int_{CD} p_c dV$. Together with the gas equation:

$$p_c = (1/V) m_c R_o T_c \quad \textbf{(1)}$$

where T_c is the in-cylinder gas temperature, equation (1) can be solved using the Runge-Kutta method. Once the in-cylinder gas temperature is known, the in-cylinder gas pressure can be obtained from the gas equation.

For internal mixture preparation it is assumed that the fuel added to the cylinder charge is immediately combusted, the combustion products mix instantaneously with the rest of the cylinder charge and form a uniform mixture, and as a consequence, the air/fuel ratio of the charge diminishes continuously from a high value at the start of combustion to the final value at the end of combustion. The flow in the tube is treated as a one-dimensional flow. This means that the pressures, temperatures, and flow velocities, obtained from the solution of the gas dynamic equations, represent mean values over the

Mechanical Testing and Diagnosis, ISSN 2247 – 9635,2011 (I), Volume 1, 40-47

cross-section of the tubes. The employed software offers several sub-models to account for several possibilities of flow modeling. In this paper, the options described in the following have been selected by keeping in mind the objective of a good compromise between the speed of computation and accuracy with respect to the experimentally obtained results. Between the three optional scavenging models, available in the employed software, the perfect mixing model is chosen. The energy content of the exhaust gases is equivalent to the mean energy content of the gases in the cylinder. The gas, leaving the cylinder, has the same composition as the mixture in the cylinder. For the verification of accuracy and fine tuning of the numerical simulation model, some experimental work is done.

3. EXPERIMENTAL EQUIPMENT AND TEST PROCEDURE

The schematic diagram of the engine test bed is presented in Figure 1. The test bed consists of an engine and electro-dynamometer Zöllner A-350AC, 300kW, air flow rate meter RMG, fuel consumption dynamic measuring system AVL, UHC analyserRatfisch, NOxchemoluminiscent analyzer Thermoelectron, O2 analyzer Programmelectronic, CO analyzer Maihak, and smoke meter AVL. Using a data acquisition system the instantaneous injection pressure and needle lift, the instantaneous in-cylinder gas pressure, the temperatures of fuel, ambient air, intake air, cooling water at inflow and outflow of the engine, oil pressure and temperature, and the temperature exhaust gases are measured.

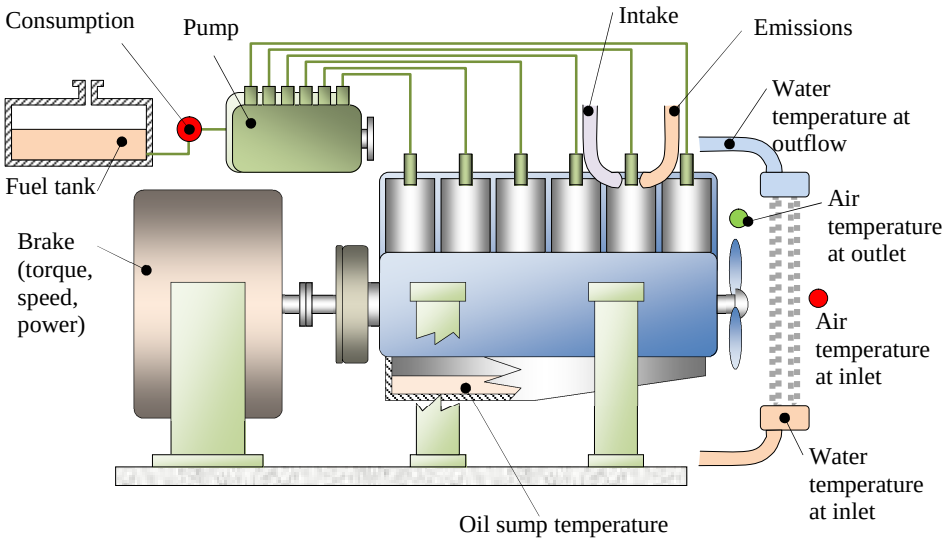

Fig. 1. The engine test bed scheme

The main specifications of the tested engine and fuel injection system are given in Table 1.

The measurements and computations of engine characteristics were performed at various engine operating regimes. The comparison was done for both tested fuels at several operating regimes at full load, especially at the peak torque and rated conditions.

The fuels under consideration are:

(i) neat mineral diesel (throughout this paper denoted as D2) and

Mechanical Testing and Diagnosis, ISSN 2247 – 9635,2011 (I), Volume 1, 40-47

(ii) neat biodiesel (throughout this paper denoted as B100 for brevity).

D2 conforms to Eur**o**pean standard EN 590. B100 is produced from rapeseed by Biogoriva, Slovenia and it conforms to European standard EN 14214. A comparison between some measured properties of D2 and B100 are given in Table 2 [5, 7].

Table 1. Test engine and injection system main specifications

Engine model	**MAN D 2566 MUM**
Enginetype	4 stroke, 6 cylinder in line, water cooled
Displacement	11 413 cm^3
Compressionratio	17.5 : 1
Bore and stroke	125 mm x 155 mm
Max Power	162 kW
Injection model	directinjection M system
Fuelinjectionpump	Bosch PES 6A 95D 410 LS 2542
Pump plunger (diameter x lift)	9.5 mm x 8 mm
Fuel tube (lengthxdiameter)	1024 mm x 1.8 mm
Injectionnozzle (numberxnozzleholediameter)	1 x 0.68 mm

Table 2. Diesel and biodiesel properties

Fuel	**D2**	**B100**
Density @ 20 ^oC (kg/m^3)	828	878
Soundvelocity @ 20 ^oC, 300 bar (m/s)	1430	1460
Kinematicviscosity @ 30 ^oC (mm^2/s)	3.34	5.51
Surface tension @ 30 ^oC (N/m)	0.0255	0.028
Bulkmodulusofelasticity @ 40 ^oC, 300 bar (MPa)	1600	1760
Calorificvalue (MJ/kg)	43.8	38.2
Cetanenumber	45	> 51

To verify the numerical simulation used for our engine model, presented in Figure 2, the in-cylinder gas pressure, the engine power and the effective specific fuel consumption were measured at various engine operating regimes.

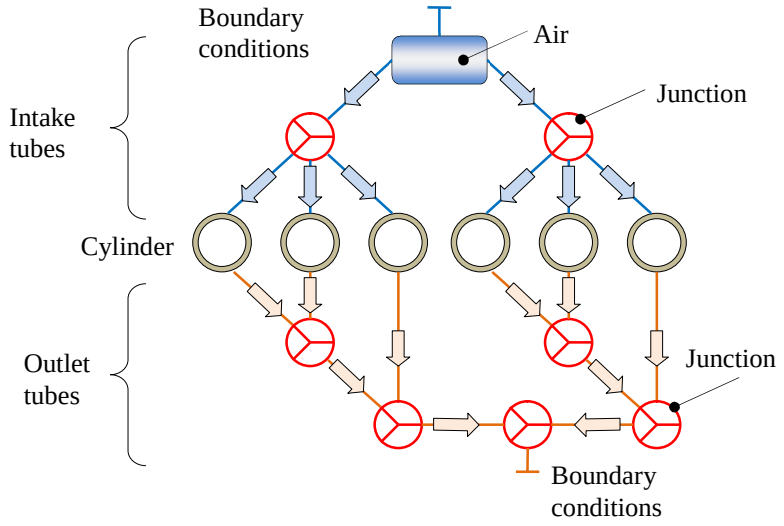

Fig. 2. The engine model for numerical simulation

4. RESULTS AND DISCUSSION

To analyze the influence of fuel properties on bus diesel engine characteristics, the most important injection and combustion characteristics, obtained with B100 and D2, are compared and discussed.

Engine performance and harmful emissions are measured at various engine regimes [8]. Because of a very good agreement between numerical and experimental results, Figure 3 shows the numerically determined engine effective power and torque and effective specific fuel consumption, only.

One can see from Figure 4 that relative NO_x emission is practically the same at all engine speeds except at very low speed where it decreases with increasing engine speed. On the other hand, the NO_x emission (not relative) generally increases with higher engine speed. This is partially due to the gas flow motion within cylinder under higher engine speed, which leads to a faster mixing between fuel and air, and a shorter ignition delay. Consequently, the reaction time of each engine cycle is reduced causing an earlier and higher in-cylinder gas temperature peak. By using B100 this effect is even more evident.

Figure 5 shows the injection pressure, needle lift, in-cylinder gas pressure and temperature, and heat release rate by using B100 and D2 fuels at peak torque conditions. Injection pressure and needle lift are determined experimentally; in-cylinder gas pressure and temperature and heat release rate are obtained by numerical simulation. The differences in pressure, when B100 and D2 are used, are almost negligible. However, differences are observed for in-cylinder gas temperature and in heat release rate. The in-cylinder gas temperature and heat release rate are lower by using B100 considerably and their peak values are advanced with respect to D2. When using B100, an earlier needle lift (advanced injection timing) was observed. This is due to higher viscosity, bulk modulus and sound velocity of B100. A higher bulk modulus leads to more rapid pressure wave propagation from the pump to the needle nozzle and an earlier needle lift. Higher viscosity of B100 leads to reduced fuel losses during injection process, to faster evolution of pressure and thus to advanced injection timing.

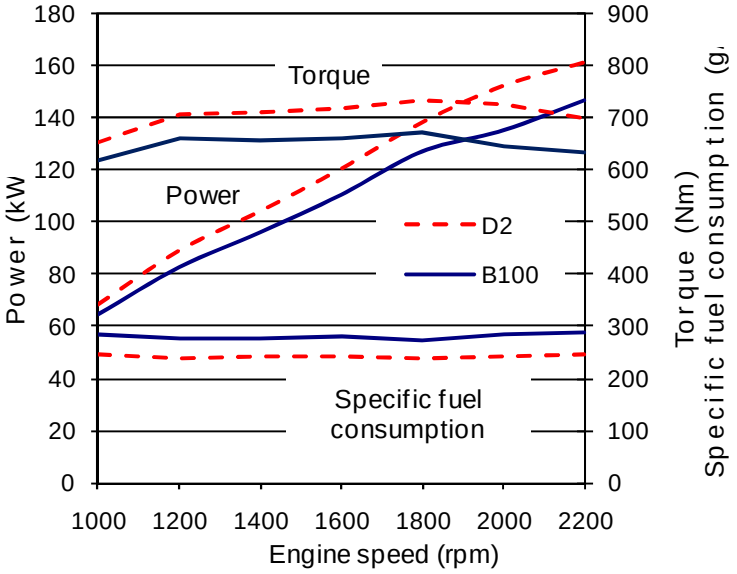

Fig. 3. Effective power and torque, injected fuel mass and specific fuel consumption (numeric)

Mechanical Testing and Diagnosis, ISSN 2247 – 9635,2011 (I), Volume 1, 40-47

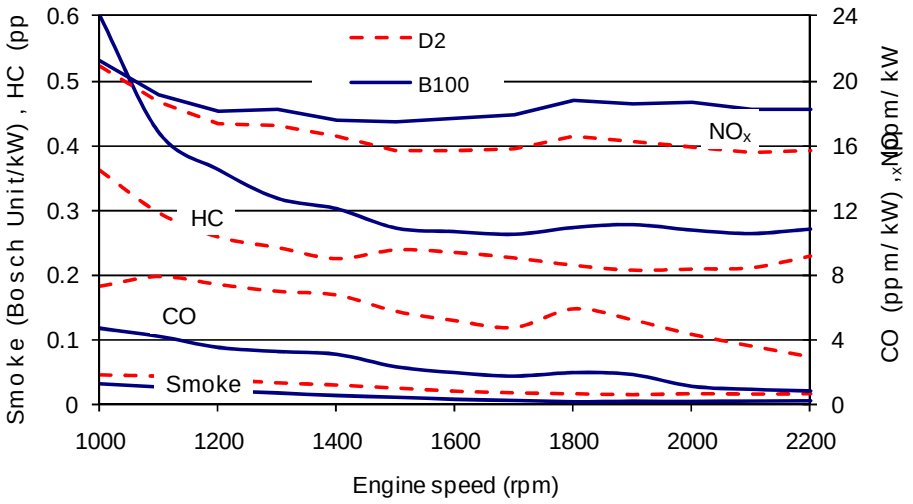

Fig. 4. Harmful relative emissions at full load conditions (experiment)

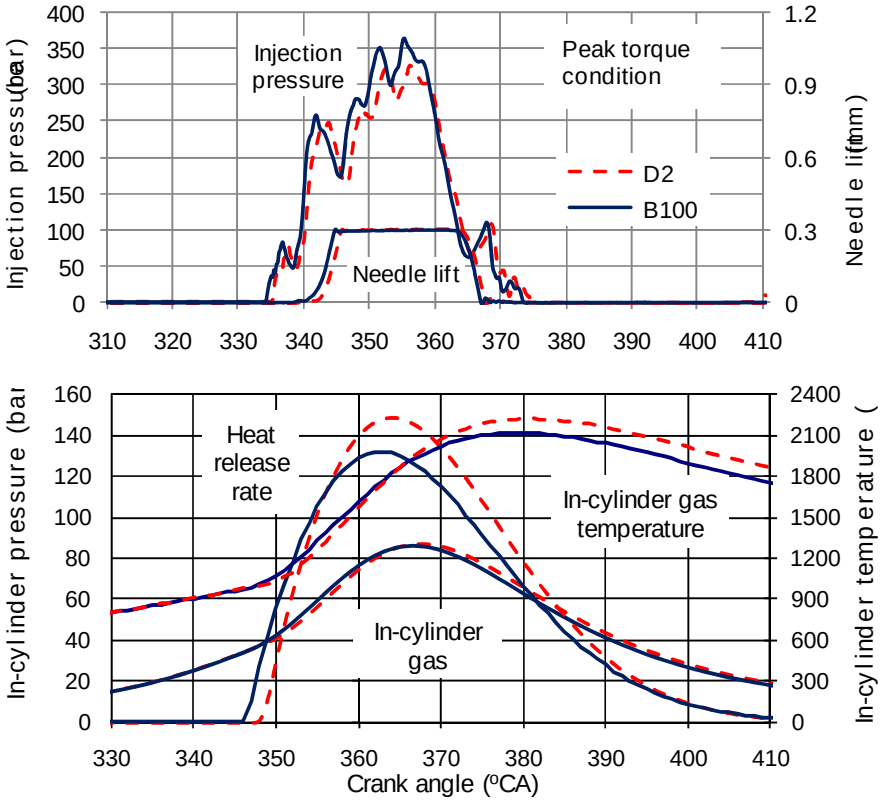

Figure 5. Injection and combustion characteristics at peak torque conditions

From Figure 6, one can see that ignition delay for B100 is always lower than that of D2. The ignition quality of a fuel is usually characterized by its cetane number. B100 has a higher cetane number and therefore exhibits a shorter ignition delay period. This results in lower exhaust gas temperatures and higher engine coolant and oil temperatures.

The ignition delay is mainly controlled by the mixture temperature, vapor, and oxygen concentration. This is especially true for the temperature at the point of injection start. Thus, a shorter ignition delay of B100 is significantly influenced by higher in-cylinder gas temperature at the beginning of injection. However, shorter ignition delay is making the atomization of the biodiesel difficult due to the higher kinematic viscosity and surface tension of biodiesel.

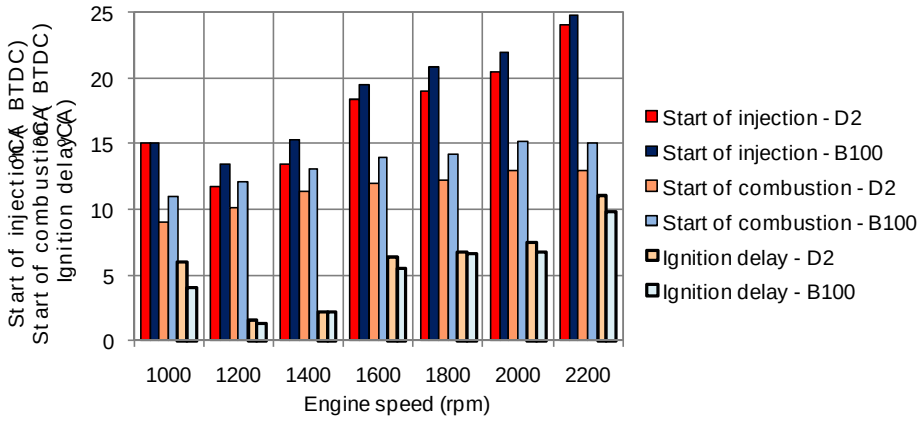

Fig. 6. Start of injection and combustion, ignition delay at full load conditions

5. CONCLUSION

By using experiments and numerical simulation, the relationships among fuel properties and engine emissions through the injection and combustion characteristics are analyzed. The findings are as follows:

- Higher density, viscosity, velocity of sound and bulk modulus of B100 and lower vapor content cause the advanced injection timing and higher injection pressure.
- The advanced injection timing causes the increase of the in-cylinder gas pressure, in-cylinder gas temperature, and an earlier rise of the heat release rate.
- The higher injection pressure, higher oxygen content and other fuel properties of B100 results in lower smoke and CO emissions and in a slightly higher HC emission. The results show that earlier appearance of temperature and heat release rate maximums prolongs the period with conditions favourable for NO_x formation.

REFERENCES

[1] **Purushothaman, K., Nagarajan, G.,** 2009, Performance, emission and combustion characteristics of a compression ignition engine operating on neat orange oil, *Renew Energy*, 34, pp. 242–245.

[2] **Balat, M., Balat, H.,** 2010, Progress in biodiesel processing. *Appl Energy*, 87, pp. 1815–1835.
[3] **Park SH, Yoon SH, Lee CS.,** 2010, Effects of multiple-injection strategies on overall spray behavious, combustion, and emissions reduction characteristics of biodiesel fuel, *Appl Energy*, http://dx.doi.org/10.1016/j.apenergy.2010.07.024.
[4] **Leung, D., Y., C., Wu X, Leung, M., K., H.,** 2010, A review on biodiesel production using catalyzed transesterification, *Appl Energy*, 87, pp.1083–1095.
[5] **Kegl, B.,** 2006, Numerical analysis of injection characteristics using biodiesel fuel, *Fuel*, 85, pp. 2377–2387.
[6] **Ganapathy, T., Murugesan K, Gakkar, P.,** 2009, Performance optimization of Jatropha biodiesel engine model using Taguchi approach. Appl Energy, 86, pp. 2476–2486.
[7] **Kegl, B.,** 2008, Effects of biodiesel on emissions of a bus diesel engine. BioresourTechnol, pp. 99:863–873.
[8] **Kegl, B.,** 2006, Experimental Investigation of Optimal Timing of the Diesel Engine Injection Pump Using Biodiesel Fuel, *Energy Fuels*, 20, pp. 1460–1470.